Heliyon 10 (2024) e28488

Contents lists available at ScienceDirect

Heliyon

journal homepage: www.cell.com/heliyon

Research article

Hyperthermia improves gemcitabine sensitivity of pancreatic cancer cells by suppressing the EFNA4/β-catenin axis and activating dCK

Qiaoxian He [a,b], Yangyang Zheng [a,b], Lei Lu [a,b], Hongzhang Shen [a,b], Weigang Gu [a,b], Jianfeng Yang [a,b,c,d,e], Xiaofeng Zhang [a,b,c,d,e], Hangbin Jin [a,b,c,d,e,*]

[a] *The Fourth School of Clinical Medicine, Zhejiang Chinese Medical University, Hangzhou, 310053, Zhejiang, PR China*
[b] *Department of Gastroenterology, Affiliated Hangzhou First People's Hospital, School of Medicine, Westlake University, Hangzhou, 310006, Zhejiang, PR China*
[c] *Key Laboratory of Integrated Traditional Chinese and Western Medicine for Biliary and Pancreatic Diseases of Zhejiang Province, Hangzhou, 310006, Zhejiang, PR China*
[d] *Hangzhou Institute of Digestive Diseases, Hangzhou, 310006, Zhejiang, PR China*
[e] *Key Laboratory of Clinical Cancer Pharmacology and Toxicology Research of Zhejiang Province, Hangzhou, 310006, Zhejiang, PR China*

ARTICLE INFO

Keywords:
Pancreatic cancer
Gemcitabine
Hyperthermia
dCK
EFNA4

ABSTRACT

Background: Previously, our investigations have underscored the potential of hyperthermia to improve the therapeutic efficacy of gemcitabine (GEM) in pancreatic cancer (PC). Nonetheless, the precise underlying mechanisms remain elusive.

Methods: We engineered two GEM-resistant PC cell lines (BxPC-3/GEM and PANC-1/GEM) and treated them with GEM alongside hyperthermia. The impact of hyperthermia on the therapeutic potency of GEM was ascertained through MTT assay, assessment of the concentration of its active metabolite dFdCTP, and evaluation of deoxycytidine kinase (dCK) activity. Lentivirus-mediated dCK silencing was further employed to validate its involvement in mediating the GEM-sensitizing effect of hyperthermia. The mechanism underlying hyperthermia-mediated dCK activation was explored using bioinformatics analyses. The interplay between hyperthermia and the ephrin A4 (EFNA4)/β-catenin/dCK axis was investigated, and their roles in GEM resistance was further explored via the establishment of xenograft tumor models in nude mice.

Results: Hyperthermia restored dCK expression in GEM-resistant cell lines, concurrently enhancing GEM sensitivity and fostering DNA damage and cell death. These observed effects were negated by dCK silencing. Regarding the mechanism, hyperthermia activated dCK by down-regulating EFNA4 expression and mitigating β-catenin activation. Overexpression of EFNA4 activated the β-catenin while suppressing dCK, thus diminishing cellular GEM sensitivity—a phenomenon remediated by the β-catenin antagonist MSAB. Consistently, *in vivo*, hyperthermia augmented the therapeutic efficacy of GEM on xenograft tumors through modulation of the ephrin A4/β-catenin/dCK axis.

Conclusion: This study delineates the role of hyperthermia in enhancing GEM sensitivity of PC cells, primarily mediated through the suppression of the EFNA4/β-catenin axis and activation of dCK.

* Corresponding author. Department of Gastroenterology, Affiliated Hangzhou First People's Hospital, School of Medicine, Westlake University, Hangzhou, 310006, Zhejiang, PR China.
E-mail address: jhbhzsy@163.com (H. Jin).

https://doi.org/10.1016/j.heliyon.2024.e28488
Received 12 December 2023; Received in revised form 20 March 2024; Accepted 20 March 2024
Available online 25 March 2024

1. Introduction

According to Global Cancer Statistics, in 2020, pancreatic cancer (PC) afflicted 495,773 individuals worldwide, with 466,003 succumbing to the disease worldwide [1], highlighting its alarming mortality rates. The most prevalent (>80%) and deadly form of PC is pancreatic adenocarcinoma (PAAD) [2]. Despite advancements leading to bolstered survival rates across various cancers, PC remains a formidable challenge, characterized by its frequent diagnosis at an advanced stage, resulting in a dismal 5-year survival rate of under 5% [3]. The terrible treatment outcome can largely be attributive to the belated diagnosis, depriving patients of the opportunity for curative interventions [4].

Gemcitabine (GEM; 2′,2′-difluoro-2′-deoxycytidine), a pyrimidine nucleoside analogue renowned for its capacity to induce DNA damage, apoptosis, and cell cycle perturbation, has long held the mantle as the first-line chemotherapy agent for locally advanced and metastatic PC [5–7]. However, the efficacy of GEM is compromised by the inherent propensity of PC cells to develop resistance, a phenomenon exacerbated by the inadequate penetration and delivery of drugs through the dense and poorly vascularized tumor stroma [8]. This acquisition of GEM resistance stands as a significant barrier to improving patient outcomes in clinical practice, thereby accentuating the urgent need to surmount this hurdle.

Hyperthermia, a form of thermotherapy elevating the temperature of targeted body region or the entire body to 41–45 °C, holds promise in selectively targeting cancer cells while preserving the integrity of surrounding healthy tissues. Moreover, it has been recognized for its capacity to potentiate the efficacy of chemotherapy and radiotherapy [9]. Our research team has previously demonstrated the effectiveness of hyperthermia (41°C–43 °C) in augmenting production of 2',2'-difluorodeoxycytidine triphosphate (dFdCTP), the main active metabolite of GEM [10]. Furthermore, we have found hyperthermia's capacity of enhancing GEM-mediated apoptosis induction, disrupting cell cycle [11], and curbing the metastatic potential of PC cells [12]. The enzymatic conversion of GEM into dFdCTP, pivotal for impeding DNA synthesis and halting cell cycle progression at early S phase, necessitates phosphorylation by deoxycytidine kinase (dCK) [13,14]. Nonetheless, the question of whether hyperthermia can potentiate GEM sensitivity in PC cells warrants further validation. Additionally, exploring the potential modulation of dCK activity by hyperthermia, along with the intricate molecular mechanisms underlying this regulatory process, presents an intriguing avenue for future investigation. Such endeavors promise to enrich our comprehension of the underlying mechanisms governing the therapeutic efficacy of hyperthermia, thereby advancing our strategies for combating PC.

Through transcriptome analysis utilizing hyperthermia-related datasets sourced from the GEO system (https://www.ncbi.nlm.nih.gov/gds/), our investigation pinpointed ephrin A4 (EFNA4) as a prominent factor significantly influenced by hyperthermia in the context of cancer treatment. EFNA4, an important member of the ephrins family, has been intricately associated with both developmental processess and tumorigenesis [15]. Notably, previous research has implicated EFNA4 in the activation of the renown oncogenic protein β-catenin, thereby potentiating the malignant characteristics of hepatocellular carcinoma cells [16]. Importantly, the β-catenin signaling has been implicated in conferring heightened resistance to GEM in PC cells [7,17]. Hence, we were compelled to explore whether the EFNA4/β-catenin axis might exert an influence on dCK activity and GEM resistance in PC. Given these insights, our study was designed to investigate the interplay between hyperthermia, the EFNA4/β-catenin axis, and dCK activity in the context of GEM resistance. To this end, we established two GEM-resistant PC cell lines to examine the multifaceted dynamics underlying this intricate relationship.

2. Materials and methods

2.1. Establishment of GEM-resistant PC cell lines

Two PC cell lines BxPC-3 (Cat. No. TCHu 12, RRID: CVCL_0186) and PANC-1 (Cat. No. SCSP-535, RRID:RRID: CVCL_0480) were procured from National Collection of Authenticated Cell Cultures (Shanghai, China). Both cell lines were authenticated using short tandem repeat profiling and were free of mycoplasma contamination. These cell lines were cultured in Dulbecco's modified Eagle medium supplemented with 10% fetal bovine saline and 1% antibiotics, and maintained in a humidified incubator at 37 °C and 5% CO_2. To establish stable GEM-resistant cell lines, the parental cells underwent a regimen of escalating GEM exposure. Initially, cells were subjected to continuous treatment with 5 μg/mL of GEM for a duration of 6 d. Subsequently, the cells were continuously exposed to incrementally higher concentrations of GEM (10, 15, 20 μg/mL) for 6 d each. Following this gradient concentration induction protocol, the harvested cells were deemed resistant to GEM and designated as BxPC-3/GEM and PANC-1/GEM cell lines. These GEM-resistant cell lines were further cultured in the medium supplemented with 10 μg/mL of GEM to perpetuate and sustain their drug resistance phenotype.

2.2. Cell treatment

To induce hyperthermia, BxPC-3/GEM and PANC-1/GEM cells were subjected to incubation in a 43 °C water bath for 1 h. Lentiviral vectors were obtained from Genomeditech (Shanghai) Co., Ltd. (Shanghai, China), including the gene-suppressive lentivirus of pLV [shRNA]-dCK1, 2, 3#, gene-overexpressing lentivirus pLV[Exp]-EFNA4, pLV[Exp]-dCK, as well as their corresponding negative control (NC) lentivirus. The lentiviral infection dose for cell transduction was 7.19×10^8 IU/mL, and stably infected cells were selected using puromycin. The specific shRNA sequences, with a loop sequence of CTCGAG, inserted into the lentiviral vectors are detailed in Table 1. For the suppression of β-catenin suppression, cells were treated with the β-catenin-specific antagonist MSAB (Cat. No.

53581ES08, Yeasen Biotechnology Co., Ltd., Shanghai, China).

2.3. Detection of dFdCTP by reverse phase high-performance liquid chromatography (RP-HPLC)

The detection of active metabolite of GEM, difluorodeoxycytidine triphosphate (dFdCTP), within cells was detected using a Shimadzu 20AT HPLC System and a Zhida N2000 Chromatography Workstation. Detailed procedures for this analysis were meticulously followed as outlined in our previous publication [10].

2.4. 3-(4, 5-dimethylthiazol-2-yl)-2, 5-diphenyltetrazolium bromide (MTT) assay

To assess the concentration-dependent cytotoxicity of GEM, BxPC-3/GEM and PANC-1/GEM cells were seeded in 96-well culture plates at a density of 5000 cells per well. Subsequently, 100 μL of medium containing varying concentrations of GEM (0, 5, 10, 15, 20, 25 μg/mL) was added to each well. When applicable, cells were subjected to hyperthermia at 43 °C before being cultured for an additional 2 h. Following this, MTT solution (5 mg/mL, Beyotime Biotechnology Co., Ltd., Shanghai, China) was added to all wells, followed by a further 4-h incubation. The formed formazan crystals were dissolved by adding dimethyl sulfoxide solution and shaken at low speed for 10 min to ensure complete dissolution. The relative viability of cells was determined by measuring the absorbance at 490 nm using a Molecular Devices microplate reader.

To evaluate alterations in cell proliferation activity, BxPC-3/GEM and PANC-1/GEM cells, with or without GEM treatment at a concentration of 14 μg/mL, were seeded in 96-well plates at a density of 2000 cells per well. After 48 h of incubation, MTT solution (5 mg/mL, Beyotime Biotechnology Co., Ltd., Shanghai, China) was added to all wells to assess cell proliferation. Subsequent steps were performed following the procedures described in the cytotoxicity tests aforementioned.

2.5. Reverse transcription quantitative polymerase chain reaction (RT-qPCR)

Total cellular RNA was extracted using the TRIzol reagent (Invitrogen, Thermo Fisher Scientific, Rockford, IL, USA), and cDNA synthesis was carried out using the PrimeScript RT Reagent Kit (Takara Holdings Inc., Kyoto, Japan). Subsequently, real-time qPCR analysis was performed employing the Premix Ex Taq master mix (Takara), following the manufacturer's instructions. Glyceraldehyde-3-phosphate dehydrogenase (GAPDH) served as the internal loading control, and the relative expression of EFNA4 and dCK mRNAs was determined utilizing the $2^{-\Delta\Delta Ct}$ method. Primer sequences utilized for amplification are provided in Table 2.

2.6. Western blot (WB) analysis

The BxPC-3/GEM and PANC-1/GEM cells were lysed in RIPA Lysis Buffer (Beyotime), and the lysates were centrifuged at 10,000 *g* for 5 min to collect the supernatant. Protein concentration was determined utilizing the Pierce™ BCA Detection Kit (Thermo Fisher Scientific). Equal amounts of protein sample (20 μg) were subjected to sodium dodecyl sulfate-polyacrylamide gel electrophoresis and transferred onto the polyvinylidene fluoride membranes. Following transfer, the membranes were blocked by 5% bovine serum albumin and subsequently incubated overnight at 4 °C with primary antibody solutions, appropriately diluted. This was succeeded by incubation with the secondary antibody at room temperature for 1 h. Protein signals were visualized using the Super ECL Detection Reagent (Yeasen Biotechnology), with the GAPDH protein band serving as the internal loading for normalization. The primary antibodies employed were against dCK (CSB-PA283493, CUSABIO Biotech Co., Ltd., Wuhan, Hubei, China), EFNA4 (#500–11154, Thermo Fisher Scientific), β-catenin (CSB-PA00174A0Rb, CUSABIO Biotech) and GAPDH (AF1186, Beyotime). Horseradish peroxidase (HRP)-conjugated goat anti-rabbit IgG (H + L) (A0208, Beyotime) served as the secondary antibody.

2.7. Immunofluorescence staining

Cells were seeded in 24-well plates at 1×10^5 cells per well and subjected to treatment with GEM (14 μg/mL) in conjunction with hyperthermia (43 °C). Following treatment, the cells were fixed with 4% paraformaldehyde for 10 min, penetrated with 0.1% Triton X-100 for 5 min, and subsequently incubated with the Alexa Fluor® 647 fluorescence-conjugated γ-H2AX (1: 50, ab195189, Abcam) at 4 °C overnight. Nuclear DNA was stained by 4′, 6-diamidino-2-phenylindole (DAPI). Subsequently, the γ-H2AX-positive cells were observed under the fluorescence microscopy.

Table 1
shRNA sequences of dCK.

	Sequence
pLV[shRNA]-dCK 1#	GCAGAGAAACCTGTATTATTTCTCGAGAAATAATACAGGTTTCTCTGC
pLV[shRNA]-dCK 2#	GAGACATGCTTACATAGAATACTCGAGTATTCTATGTAAGCATGTCTC
pLV[shRNA]-dCK 3#	GCAGCCTGCTATAAAGTTAAACTCGAGTTTAACTTTATAGCAGGCTGC

Note: shRNA, short hairpin RNA; dCK, deoxycytidine kinase.

Table 2
Primer sequences for qPCR analysis.

	Forward primer (5'-3')	Forward primer (5'-3')
GAPDH	GTCTCCTCTGACTTCAACAGCG	ACCACCCTGTTGCTGTAGCCAA
EFNA4	TTGAGGCTCCAGGTGTCTGTCT	CAATGCTCCATCTTGTCGGTCTG
dCK	AGTGGTTCCTGAACCTGTGCC	GACCATCGTTCAGGTTTCTCTAC

Note: qPCR, quantitative polymerase chain reaction; GAPDH, glyceraldehyde-3-phosphate dehydrogenase; EFNA4, ephrin A4; dCK, deoxycytidine kinase.

2.8. Terminal deoxynucleotidyl transferase (TdT)-mediated dUTP nick end labeling (TUNEL)

Apoptosis of cells was assessed utilizing the One-Step TUNEL In-Situ Cell Apoptosis Detection Kit (Procell Life Science & Technology Co., Ltd., Wuhan, Hubei, China). Briefly, cells were fixed with 4% paraformaldehyde, penetrated with 0.1% Triton X-100, and subsequently reacted with 100 μL of TdT Equilibration Buffer at 37 °C for 30 min. This was followed by incubation in the dark with 50 μL of Working Solution in wet box at 37 °C for 60 min. Nuclear staining was accomplished by incubating the cells with DAPI in the dark for 5 min. Following this, the cell slides were sealed and subjected to observation under a fluorescence microscope.

2.9. Colony formation assay

Cells were seeded in six-well plates at a density of 500 cells per well and subjected to treatment with GEM (14 μg/mL) in conjunction with hyperthermia (43 °C). Following a two-week incubation period, the cells were fixed for 30 min and stained with 0.1% crystal violet for 15 min. The number of formed colonies was calculated under a microscope.

2.10. TOP Flash/FOP flash luciferase reporter assay

To assess the β-catenin-mediated transcriptional activity of TCF/LEF, the TOP Flash reporter vector (D2501, Beyotime) was utilized, with the FOP Flash reporter vector containing mutant TCF/LEF binding sequences (D2503, Beyotime) serving as the NC. These reporter vectors were transfected into the cells using Lipofectamine 2000 (Thermo Fisher Scientific). After 24 h, luciferase activity within cells was examined utilizing the Firefly Luciferase Reporter Gene Detection Kit (Beyotime). The relative activity of the β-catenin signaling was evaluated by analyzing the ratio of TOP Flash/FOP Flash activity.

2.11. Tumor xenograft models

Forty-eight female BALB/c nude mice, aged 6 weeks, were obtained from SJA Laboratory Animal Co., Ltd. (Hunan, China). The animal study protocol was approved by the Animal Ethics Committee of Affiliated Hangzhou First People's Hospital, School of Medicine, Westlake University (Approval No. 2022-1013), and all procedures adhered strictly to the guidelines outlined in the Care and Use of Laboratory Animals (NIH, Bethesda, MD, USA). To minimize animal sacrifice, only the PANC-1/GEM cell line was used for animal the trials. In brief, approximately 5×10^6 PANC-1/GEM cells were subcutaneously injected into the nude mice. The length (L) and width (W) of the palpable tumor were measured using a caliper, and tumor volume (V) was calculated by the formula: $V = (L \times W^2)/2$. Tumor volume was monitored.

2.12. Assessment of the hyperthermia-mediated GEM treatment efficacy

When the tumor volume reached approximately 100 mm3, the mice were intraperitoneally injected with GEM (20 mg/kg) once a week [18]. Concurrently, mice designated for MSAB treatment received intraperitoneal injections of MSAB at a dose of 10 mg/kg [19]. Subsequently, 4 h following GEM treatment, the tumor-bearing mice underwent local exposure to a 13.56 MHz radiofrequency wave utilizing a radiofrequency hyperthermal equipment specifically designed for rodents, administered at an energy dose of 2 W for 1 min [20]. The weekly alterations in tumor volume were diligently monitored. After four weeks of GEM treatment, the mice were sacrificed by intraperitoneal injection of an overdose of pentobarbital sodium, and the xenograft tumors were collected for further analysis. The tumor inhibition rate was calculated based on tumor weight, using the following formula: rate (%) = (1 - T/C) × 100, where C (Control) represents the tumor weight of the pLV[Exp]-NC group, and the other groups are considered as T (Experimental groups).

2.13. Immunohistochemistry (IHC)

The harvested xenograft tumor tissues were processed into paraffin-embedded sections (4 μm). These sections underwent dewaxing, rehydration, and heat-mediated antigen retrieval. Subsequently, they were treated with 3% H_2O_2 to block endogenous peroxidase activity, followed by blocking with 5% normal goat serum to reduce non-specific binding. The sections were then incubated overnight at 4 °C with diluted antibodies of dCK (CSB-PA283493, CUSABIO Biotech), EFNA4 (#500–11154, Thermo Fisher Scientific), and β-catenin (CSB-PA00174A0Rb, CUSABIO Biotech). Following this, the sections were incubated with the HRP-conjugated goat anti-rabbit IgG (H + L) (A0208, Beyotime) at room temperature for 1 h. Subsequently, color development was achieved using 3,3′-

diaminobenzidine for 5 min, and the tissue slides were counter-stained with hematoxylin before microscopic observation. The positive staining area, identifiable by its brown coloration under microscopy, was quantified using Image J software.

2.14. Statistics

All experimental data were derived from a minimum of three independent experiments and are presented as the mean ± standard deviation. Statistical analyses were conducted using Prism 8.0.2 (GraphPad, La Jolla, CA, USA). The dose-dependent cytotoxicity of GEM was assessed by Nonlinear fit analysis. Differences among multiple groups were evaluated using either one- or two-way analysis of variance (ANOVA), followed by the Sidak's or Tukey's multiple comparison tests. A *p*-value less than 0.05 was considered statistically significant.

3. Results

3.1. Hyperthermia enhances dCK activity in GEM-resistant PC cells

Two GEM-resistant PC cell lines BxPC-3/GEM and PANC-1/GEM were established through exposure of parental cells to escalating doses of GEM. As anticipated, compared to the parental cells, the GEM-resistant counterparts exhibited a substantial increase in the half maximal inhibitory concentration (IC50) of GEM (fold change of IC50: 1.78 in BxPC-3/GEM; 1.73 in PANC-1/GEM) as determined by the MTT assay (Fig. 1A). To induce moderate damage, a GEM concentration of 14 μg/mL was employed in subsequent experiments.

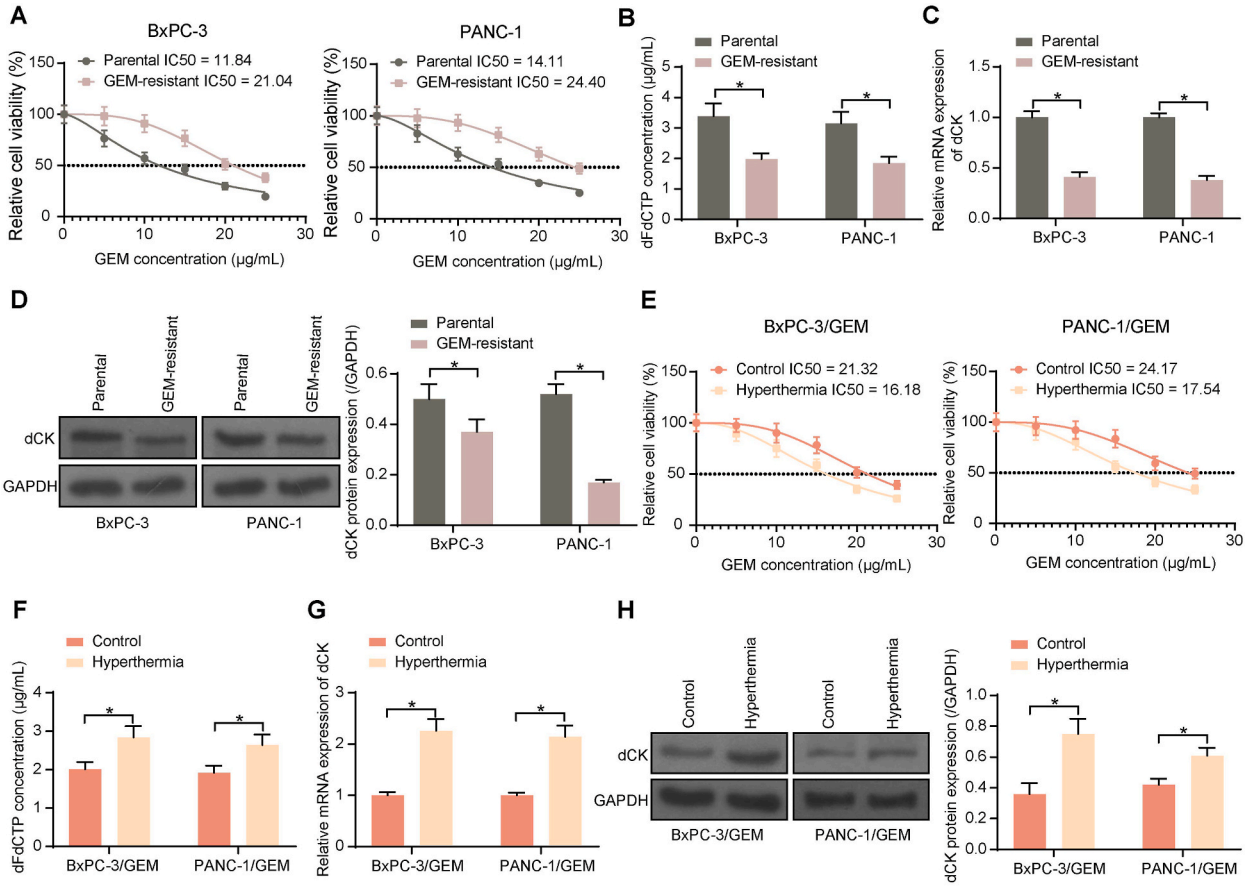

Fig. 1. Hyperthermia enhances dCK activity in GEM-resistant PC cells. A, sensitivity of parental and GEM-resistant cells to GEM examined by the MTT assay; B, dFdCTP concentration in parental and GEM-resistant cells examined by RP-HPLC detection; C-D, mRNA (C) and protein (D) levels of dCK in parental and GEM-resistant cells determined by RT-qPCR and WB assays (uncropped images of gels and blots are provided as Supplementary material), respectively; E, GEM sensitivity of the GEM-resistant cells after 43 °C hyperthermia determined by MTT assay; F, dFdCTP concentration in GEM-resistant cells after 43 °C hyperthermia examined by RP-HPLC detection; G-H, mRNA (G) and protein (H) levels of dCK in GEM-resistant cells after 43 °C hyperthermia determined by RT-qPCR and WB assays (uncropped images of gels and blots are provided as Supplementary material), respectively. The dose-dependent cytotoxicity of GEM was analyzed by Nonlinear fit (A and E). Three biological replicates were performed. Differences were compared by the two-way ANOVA followed by Sidak's multiple comparison test (B, C, D, F, G and H). *$p < 0.05$.

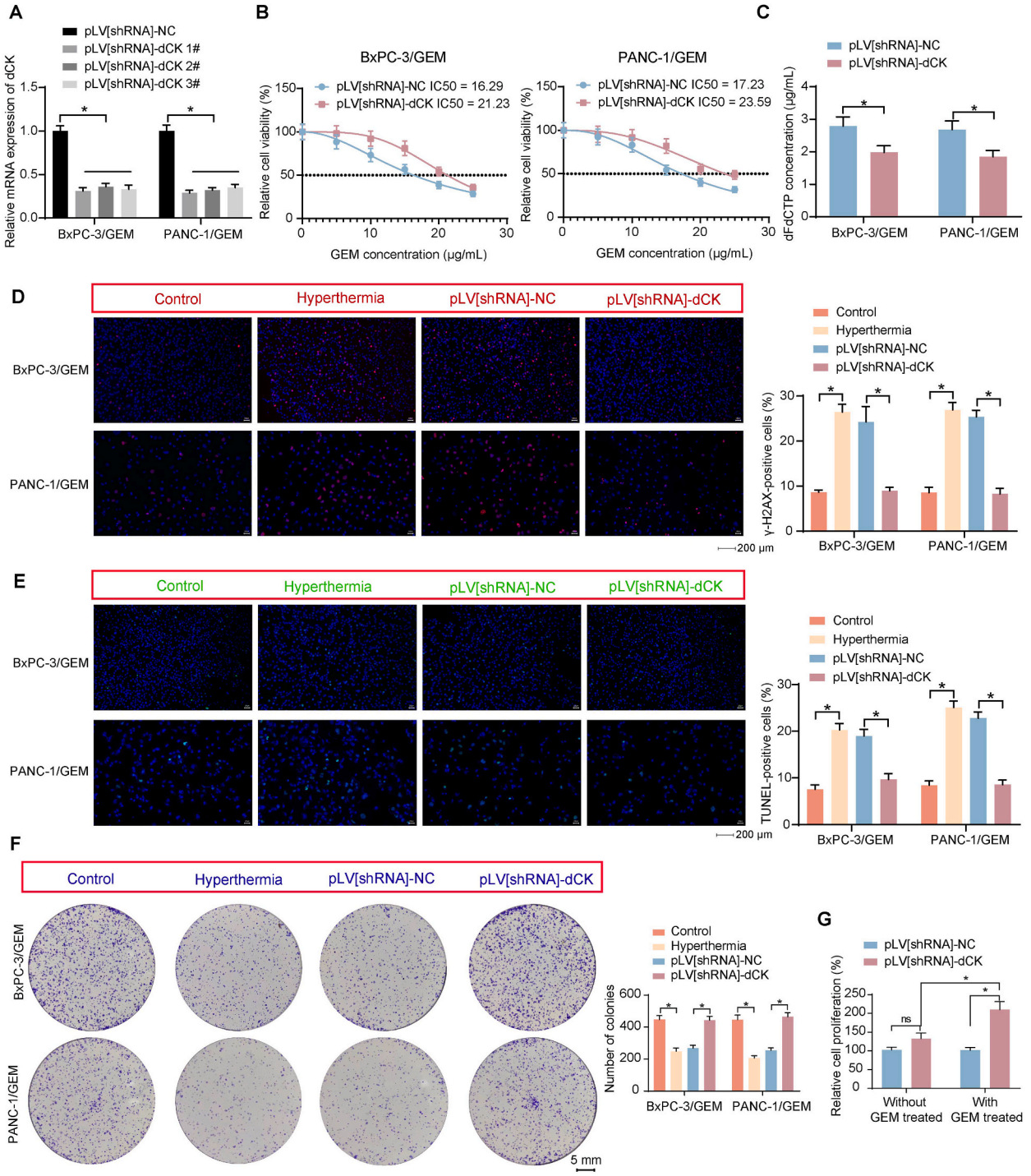

Fig. 2. The sensitizing effect of hyperthermia on GEM in PC cells depends on dCK activity. The BxPC-3/GEM and PANC-1/GEM cells were administered pLV[shRNA]-dCK, followed by GEM treatment and 43 °C hyperthermia. A, dCK-knockdown effect of pLV[shRNA]-dCK 1, 2, 3# in the two cell lines examined by RT-qPCR; B, GEM sensitivity in cells determined by MTT assay; C, dFdCTP concentration in cells examined by RP-HPLC detection; D, γ-H2AX expression in cells determined by immunofluorescence staining (scale bar = 200 μm); E, apoptosis of cells determined by TUNEL assay (scale bar = 200 μm); F, proliferation of cells analyzed by colony formation assay (scale bar = 5 mm). The BxPC-3/GEM and PANC-1/GEM cells were administered pLV[shRNA]-dCK, followed by GEM treatment or not. G, proliferation of cells determined by MTT assay. The dose-dependent cytotoxicity of GEM was analyzed by Nonlinear fit (B). Three biological replicates were performed. Differences were compared by the two-way ANOVA followed by Sidak's (C and G) or Tukey's (A, D-F) multiple comparison test. *$p < 0.05$.

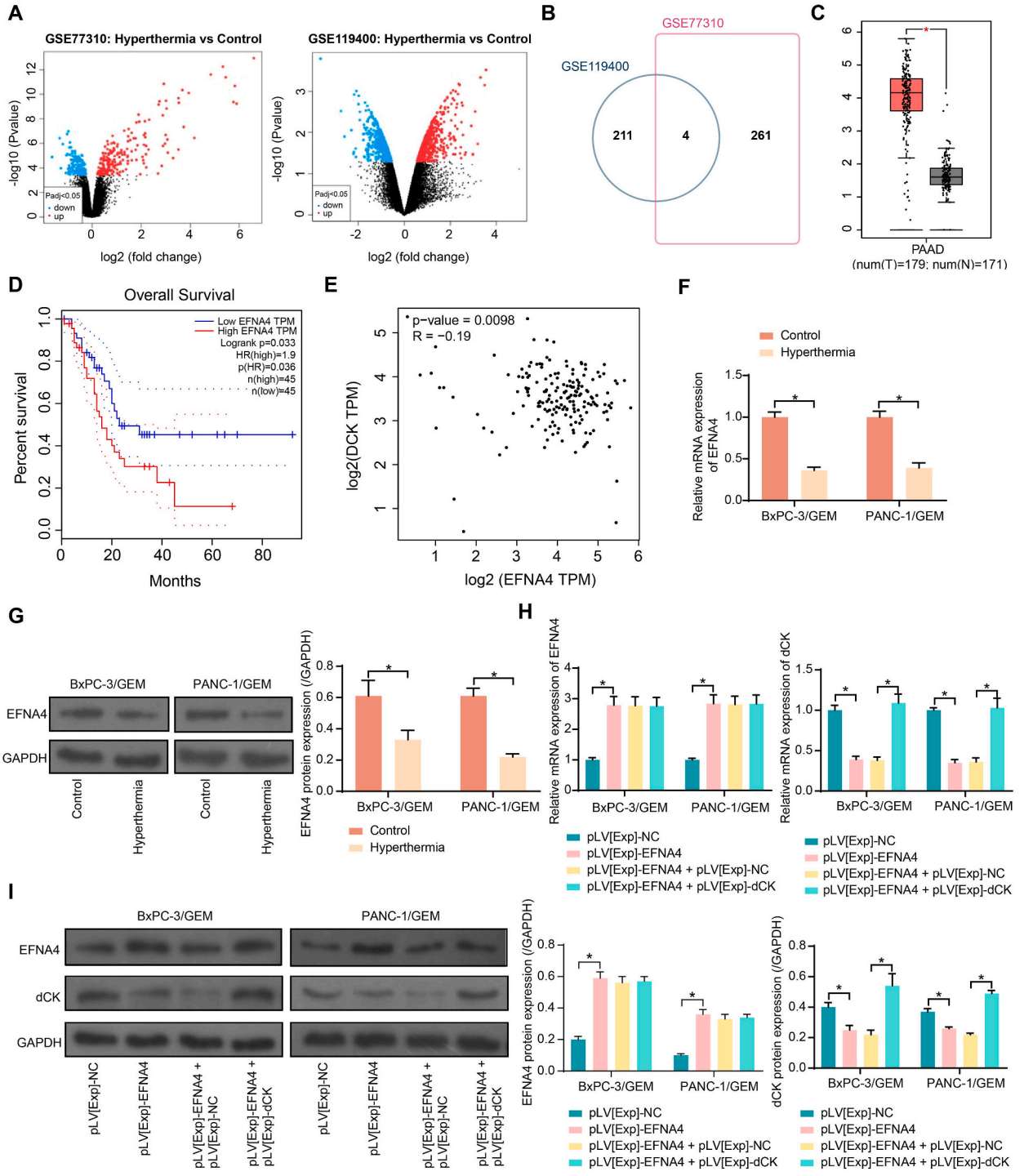

Fig. 3. Hyperthermia activates dCK by suppressing EFNA4 expression. A, volcano plots for DEGs in cancer cells after hyperthermia (screened by $p < 0.05$) in GSE77310 and GSE119400 datasets, respectively; B, intersections of the common DEGs in the two datasets; C-E, expression pattern (C), prognostic value (D) of EFNA4 and its correlation with dCK expression (E) in PAAD in the GEPIA website; F-G, mRNA (F) and protein (G) levels of EFNA4 in BxPC-3/GEM and PANC-1/GEM cells after hyperthermia determined by RT-qPCR and WB analysis (uncropped images of blots are provided as Supplementary material), respectively; H–I, mRNA (H) and protein (I) levels of EFNA4 in BxPC-3/GEM and PANC-1/GEM cells after pLV [Exp]-EFNA4 and pLV[Exp]-dCK administrations determined by RT-qPCR and WB analysis (uncropped images of blots are provided as Supplementary material), respectively. Three biological replicates were performed. Differences were compared by the two-way ANOVA followed by Sidak's (F and G) or Tukey's (H and I) multiple comparison test. *$p < 0.05$.

In this setting, it was observed that the conversion of GEM to its active metabolite dFdCTP was notably suppressed in the GEM-resistant cell lines (Fig. 1B). Additionally, a marked reduction in both dCK mRNA and protein levels was evident in the drug-resistant cells (Fig. 1C–D). Interestingly, under hyperthermic conditions at 43 °C, the sensitivity of the cells to GEM treatment was significantly increased (fold change of IC50: 0.76 in BxPC-3/GEM; 0.73 in PANC-1/GEM) (Fig. 1E). Furthermore, hyperthermia augmented the metabolic activity of GEM in these cells, as manifested by increased concentrations of dFdCTP (Fig. 1F). Moreover, the levels of dCK mRNA and protein in BxPC-3/GEM and PANC-1/GEM cells were upregulated by exposure to 43 °C hyperthermia (Fig. 1G–H).

The pivotal role of dCK in GEM sensitivity was further investigated by introducing dCK overexpression into the GEM-resistant cancer cell lines using pLV[Exp]-dCK. Successful upregulation of dCK mRNA and protein levels was confirmed by RT-qPCR and WB analysis, respectively (Supplementary Figs. S1A–B). As anticipated, dCK overexpression led to a substantial enhancement in the sensitivity of the cells to GEM, as evidenced by a significant reduction in the IC50 of GEM (fold change of IC50: 0.57 in BxPC-3/GEM; 0.66 in PANC-1/GEM) (Supplementary Fig. S1C), along with an increase in the and elevated concentration of dFdCTP (Supplementary Fig. S1D).

3.2. The sensitizing effect of hyperthermia on GEM in PC cells depends on dCK activity

To explore the involvement of dCK in the hyperthermia-mediated events, three lentivirus-carried shRNAs targeting dCK (pLV[shRNA]-dCK 1, 2, 3#) were introduced into both BxPC-3/GEM and PANC-1/GEM cells. Subsequently, the most effective shRNA, pLV[shRNA]-dCK 1#, which exhibited optimal suppression of dCK expression (Fig. 2A), was selected for subsequent experiments. These cells were then subjected to treatments involving GEM and hyperthermia. It was observed that silencing of dCK attenuated the GEM-sensitizing effect of hyperthermia, as manifested by the restoration of IC50 of GEM (fold change of IC50: 1.30 in BxPC-3/GEM; 1.37 in PANC-1/GEM) (Fig. 2B), along with a reduction in the concentration of dFdCTP (Fig. 2C).

In terms of DNA damage in BxPC-3/GEM and PANC-1/GEM cells, it was observed that positive immunofluorescence staining of γ-H2AX in cells was increased after hyperthermia, but this effect was mitigated by dCK silencing (Fig. 2D). Additionally, the TUNEL assay indicated that hyperthermia promoted GEM-induced apoptosis in cells, whereas this effect was by dCK silencing (Fig. 2E). Conversely, the proliferation of these two GEM-resistant cell lines was suppressed by hyperthermia but enhanced by dCK over-expression (Fig. 2F).

Furthermore, the impact of dCK knockdown on GEM-resistant cells in the absence of hyperthermia was assessed. Importantly, it was observed that in the absence of GEM treatment, dCK knockdown resulted in a slight increase in cell proliferation activity, although without significant differences. However, in the presence of GEM treatment, dCK knockdown significantly elevated cell proliferation activity (Fig. 2G).

3.3. Hyperthermia activates dCK by suppressing EFNA4 expression

To dissect the mechanism underlying hyperthermia-mediated dCK activation, we conducted transcriptome analysis utilizing datasets GSE119400 (hyperthermia: GSM3374164 and GSM3374165; control: GSM3374162) and GSE77310 (hyperthermia: GSM2048847, GSM2048848, GSM2048851 and GSM2048852; control: GSM2048845, GSM2048846, GSM2048849 and GSM2048850) obtained from the GEO system. Differentially expressed genes (DEGs) in cancer cells induced by hyperthermia were identified using a threshold of $p < 0.05$ (Fig. 3A). Following annotation, DEGs from both datasets were cross-referenced, revealing four intersections: HSPA1A, HSPA1B, EFNA4 and HSPB1 (Fig. 3B). Notably, among these genes, EFNA4 stands out as the only one not belonging to the heat shock protein (HSP) family, and its correlation with hyperthermia remains undefined. Interestingly, EFNA4 expression in cancer cells was significantly downregulated after hyperthermia treatment in both datasets. Subsequently, analysis from the GEPIA website (http://gepia.cancer-pku.cn/index.html) revealed that EFNA4 is significantly overexpressed in PAAD (Fig. 3C), and patients exhibiting higher EFNA4 expression (group cutoff by quartile) demonstrate lower overall survival rates (Fig. 3D). Remarkably, EFNA4 expression in PAAD displays an inverse correlation with dCK in this system (Fig. 3E). Based on these findings, we hypothesize that hyperthermia possibly suppresses EFNA4 expression to increase the dCK activity.

Building upon the hypothesis, we proceeded to investigate EFNA4 expression in the BxPC-3/GEM and PANC-1/GEM cell lines. Remarkably, hyperthermia led to a reduction in EFNA4 mRNA and protein levels in both cell lines (Fig. 3F–G). Subsequently, we introduced pLV[Exp]-EFNA4 and pLV[Exp]-dCK into the cells. RT-qPCR and WB assays revealed that pLV[Exp]-EFNA4 administration resulted in increased EFNA4 expression while simultaneously suppressing dCK expression levels. Additionally, further administration of pLV[Exp]-dCK restored dCK levels without impacting EFNA4 expression (Fig. 3H–I).

3.4. Artificial upregulation of EFNA4 and dCK affects GEM resistance of the PC cells

The GEM-resistant cell lines administered pLV[Exp]-EFNA4 and pLV[Exp]-dCK were subsequently exposed to GEM treatment and 43 °C hyperthermia. Results indicated a significant increase in the IC50 of GEM in cells upon EFNA4 overexpression (fold change of IC50: 1.40 in BxPC-3/GEM, 1.34 in PANC-1/GEM), but this effect was reversed by additional dCK upregulation (fold change of IC50: 0.68 in BxPC-3/GEM; 0.76 in PANC-1/GEM) (Fig. 4A). Moreover, the dFdCTP concentration in the cells was suppressed by EFNA4 overexpression but restored by dCK overexpression (Fig. 4B). Additional aspects revealed that EVNA4 overexpression led to a decrease in immunofluorescence staining of γ-H2AX (Fig. 4C), suppressed cell apoptosis (Fig. 4D), and enhanced colony formation ability in both GEM-resistant PC cell lines (Fig. 4E). However, these effects on cell survival and proliferation were counteracted by further dCK overexpression (Fig. 4C–E).

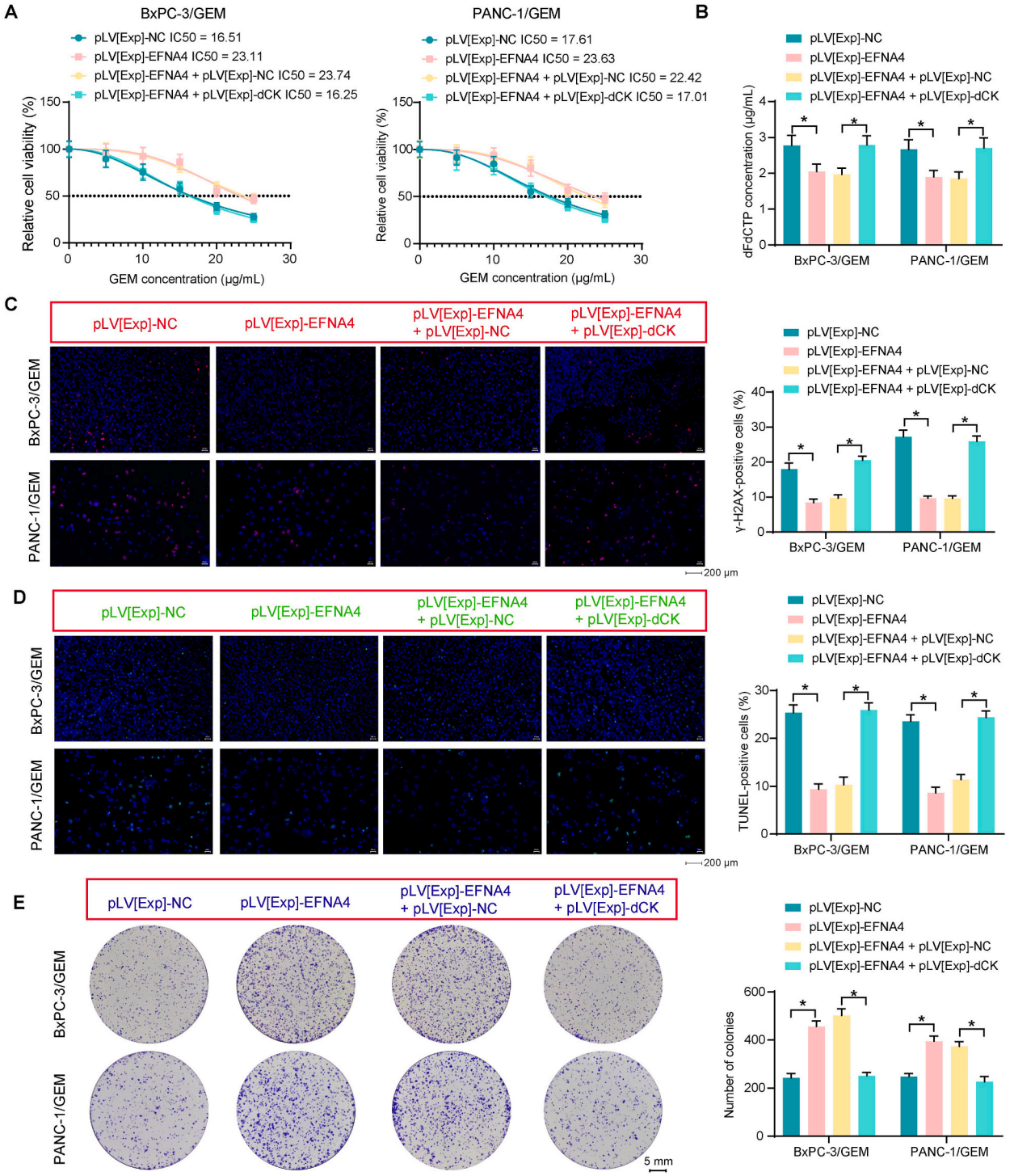

Fig. 4. Artificial upregulation of EFNA4 and dCK affects GEM resistance of the PC cells. The BxPC-3/GEM and PANC-1/GEM cells were administered pLV[Exp]-EFNA4 and pLV[Exp]-dCK, followed by GEM treatment and 43 °C hyperthermia. A, GEM sensitivity of cells determined by MTT assay; B, dFdCTP concentration in cells examined by RP-HPLC detection; C, γ-H2AX expression in cells determined by immunofluorescence staining (scale bar = 200 μm); D, apoptosis of cells determined by TUNEL assay (scale bar = 200 μm); E, proliferation of cells analyzed by colony formation assay (scale bar = 5 mm). The dose-dependent cytotoxicity of GEM was analyzed by Nonlinear fit (A). Three biological replicates were performed. Differences were compared by the two-way ANOVA followed by Tukey's multiple comparison test (B–E). *$p < 0.05$.

3.5. The suppressive effect of EFNA4 on dCK depends on the β-catenin signaling activation

EFNA4 has been previously implicated in activating the oncogenic β-catenin signaling to facilitate tumorigenesis [16]. To elucidate the potential involvement of β-catenin in the interplay between hyperthermia, EFNA4, and dCK, we investigated β-catenin activity in the two cell lines following different treatments. The findings revealed that hyperthermia significantly suppressed the protein levels of β-catenin (Fig. 5A) as well as its transcriptional activity (Fig. 5B) in both BxPC-3/GEM and PANC-1/GEM cells. Additionally, cells with artificially elevated EFNA4 levels were subjected to further treatment with MSAB. Utilizing the TOP/FOP Flash assay, we observed that the transcriptional activity of β-catenin, suppressed by hyperthermia, was restored by EFNA4 upregulation. However, this effect was then reversed upon subsequent MSAB treatment (Fig. 5C). Similarly, WB analysis demonstrated that EFNA4 upregulation increased the protein levels of β-catenin while suppressing dCK level. Conversely, further treatment with MSAB in these cells resulted in β-catenin suppression and restoration of dCK expression (Fig. 5D).

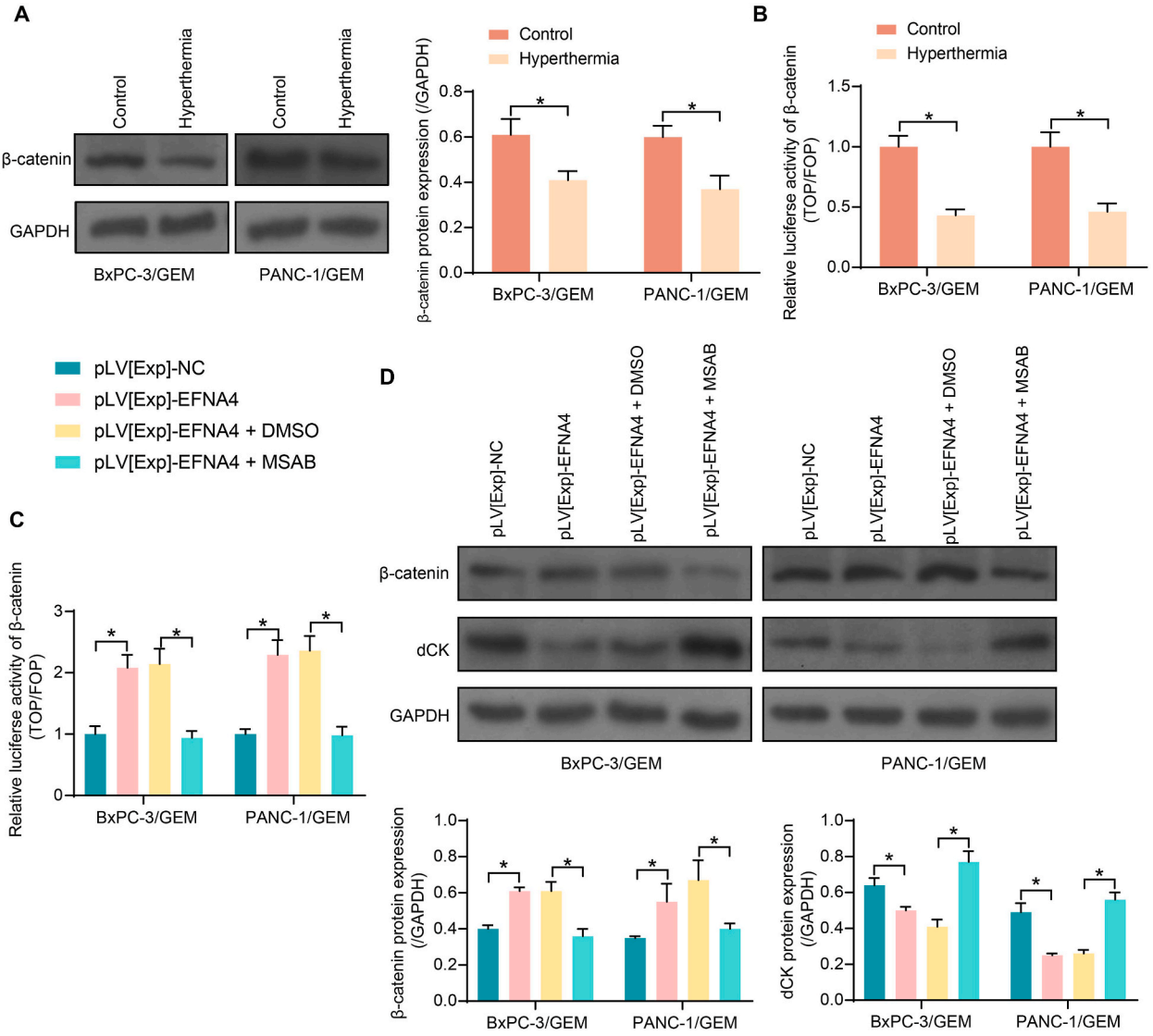

Fig. 5. The suppressive effect of EFNA4 on dCK depends on the β-catenin signaling activation. A, protein level of β-catenin in in BxPC-3/GEM and PANC-1/GEM cells after hyperthermia examined by WB analysis (uncropped images of blots are provided as Supplementary material); B, transcriptional activity of β-catenin in cells after hyperthermia determined by TOP Flash/FOP Flash luciferase reporter assay; C, transcriptional activity of β-catenin in cells after EFNA4 overexpression and MSAB treatment determined by TOP Flash/FOP Flash luciferase reporter assay; D, protein levels of β-catenin and dCK in cells after EFNA4 overexpression and MSAB treatment determined by WB analysis (uncropped images of blots are provided as Supplementary material). Three biological replicates were performed. Differences were compared by the two-way ANOVA followed by Sidak's (A–B) or Tukey's (C–D) multiple comparison test. *$p < 0.05$.

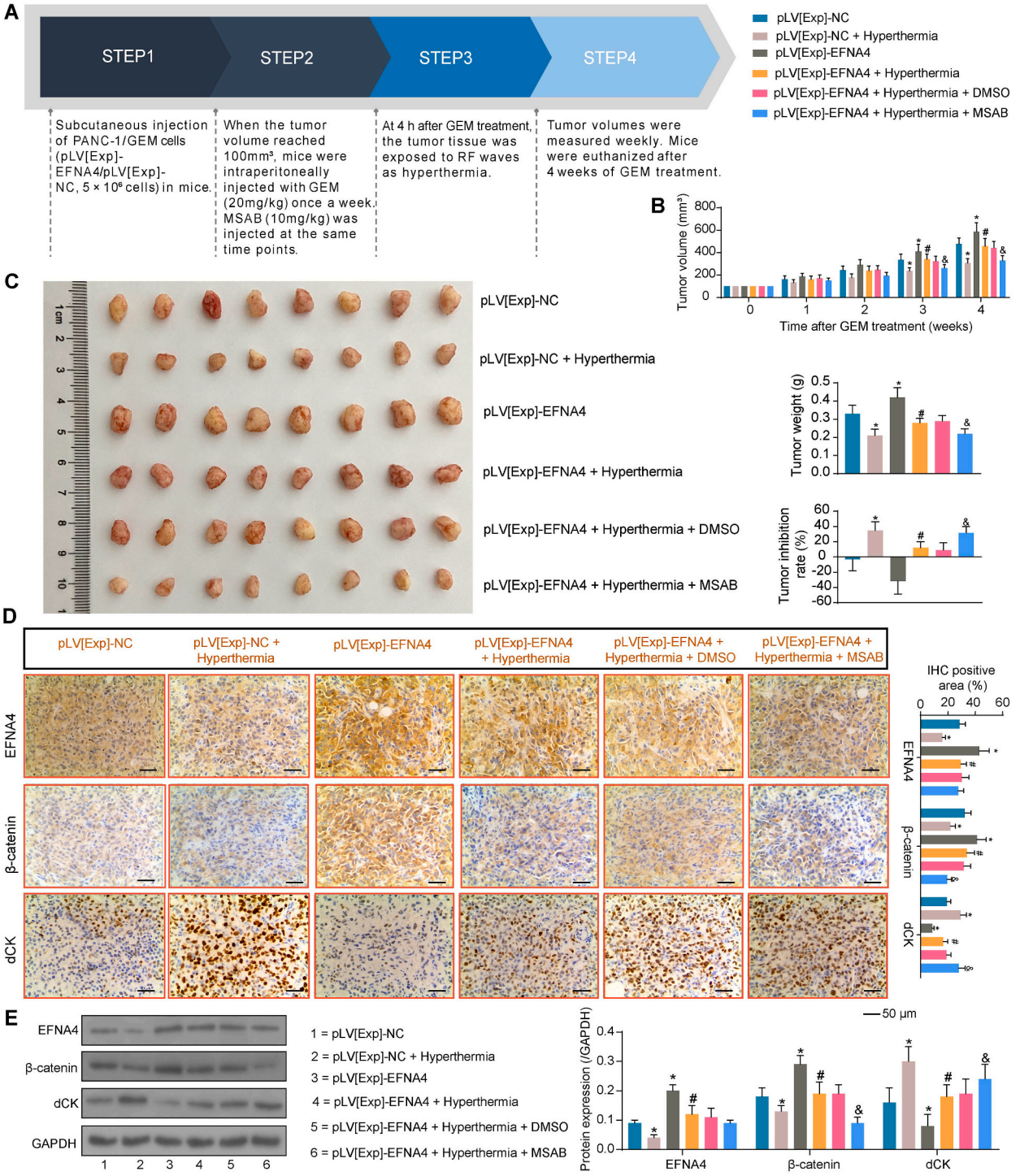

Fig. 6. Hyperthermia influences the EFNA4/β-catenin/dCK axis to affect the GEM resistance of xenograft tumors. A, a diagram for animal treatment; B, volume change of the xenograft tumors in nude mice; C, weight of xenograft tumors after four weeks of GEM treatment and the tumor inhibition rate; D-E, protein levels of EFNA4, β-catenin, and dCK in the xenograft tumor tissues examined by IHC (D) (scale bar = 50 μm) and WB (E) assays (uncropped images of blots are provided as Supplementary material). In each group, n = 8. Differences were compared by the one-way ANOVA (C) or two-way ANOVA (B and D) followed by Tukey's multiple comparison test. *$p < 0.05$ vs. the pLV[Exp]-NC group; #$p < 0.05$ vs. the pLV[Exp]-EFNA4 group; &$p < 0.05$ vs. the pLV[Exp]-NC group + Hyperthermia + DMSO group.

3.6. Hyperthermia influences the EFNA4/β-catenin/dCK axis to affect the GEM resistance of xenograft tumors

PANC-1/GEM cells stably transfected with pLV[Exp]-EFNA4 or pLV[Exp]-NC were implanted into nude mice subcutaneously to generate xenograft tumors. When the tumor volume reached approximately 100 mm^3, mice were subjected to GEM treatment, hyperthermia, and MSAB treatment (Fig. 6A). Compared to the control cells, those overexpressing EFNA4 exhibited significantly increased resistance to GEM and enhanced tumorigenic activity. Interestingly, hyperthermia mitigated drug resistance, with these effects further augmented by MSAB treatment (Fig. 6B). Moreover, changes in tumor weight paralleled those observed in tumor volume, and the tumor inhibition rate was suppressed by EFNA4 overexpression, augmented by hyperthermia, and further bolstered by MSAB (Fig. 6C). Subsequent examination of tumor tissues via IHC and WB analysis revealed that tumors formed by EFNA4-overexpressing cells displayed markedly elevated β-catenin expression but reduced dCK expression. Hyperthermia led to suppression of EFNA4 and β-catenin levels while promoting dCK expression. Additionally, MASB treatment further suppressed β-catenin expression and enhanced dCK expression to a greater extent (Fig. 6D–E).

4. Discussion

Undoubtedly, overcoming drug resistance stands as a pivotal challenge in the clinical management of PC, prompting clinicians to tirelessly seek alternative or adjunctive therapies. In our preceding investigations, we unequivocally established the GEM-sensitizing impact of hyperthermia in PC cell lines [10–12]. In the current study, we unveil that the hyperthermia executes this function by promoting dCK activity, a mechanism intricately linked with the suppression of the EFNA4/β-catenin axis.

Hyperthermia stands as a relatively moderate and safe form of thermotherapy when juxtaposed with thermal ablation, offering selective eradication of cancer cells within the tumor microenvironment characterized by low pO_2 and pH levels [9,21]. Its potential synergistic effects with chemotherapy are promising, amplifying drug cytotoxicity and inducing cell death within the heat-exposed region, all while mitigating systemic toxicity or increasing oncogenic potential [22]. Preclinical trials have consistently demonstrated the synergistic anti-tumor efficacy of chemotherapeutic agents with regional hyperthermia [23,24]. In clinical investigations, adjuvant hyperthermia in conjunction with GEM post-surgery has effectively controlled the local-regional PC [25]. In the present study, we validate the efficacy of 43 °C hyperthermia in augmenting the therapeutic impact of GEM in two established GEM-resistant PC cell lines. This augmentation is evidenced by diminished cell viability, heightened DNA damage and cell apoptosis, alongside escalated concentrations of the GEM active metabolite dFdCTP. Furthermore, we confirmed that the intensified dFdCTP production induced by hyperthermia predominantly stems from enhanced dCK activity. dCK is a kinase necessary for the polarization of GEM into its mononucleotide form for subsequent metabolism [14]. It can function as an intracellular enzyme that activates cytarabine, an antimetabolite commonly used for leukemia and non-Hodgkin's lymphoma [26]. Significantly, the protein expression of dCK has been associated with prolonged survival in PC patients subjected to surgical resection and adjuvant GEM treatment [27]. Moreover, dCK has been identified to inhibit the transcriptional activity of NF-E2 p45-related factor 2 and the transcription of antioxidant genes, ultimately resulting in reduced reactive oxygen species production and heightened GEM sensitivity [28]. Our findings, in partial accordance with those of Funamizu et al. [29], corroborate that sole dCK overexpression in GEM-resistant PC cells significantly decreased the IC50 of GEM and enhanced dFdCTP concentration. The additional observation that artificial silencing of dCK diminished the GEM sensitivity in cells supports the notion that the GEM-sensitizing effect of hyperthermia is dCK-dependent. However, the precise molecular mechanisms underlying this phenomenon remain unclear.

Hyperthermia typically influences members of the HSP family. For instance, it has been observed to upregulate HSP70 levels, thereby inactivating nuclear factor kappa B and augmenting the cytotoxicity of GEM on PC cells [30]. Additionally, hyperthermia has been shown to induce HSP27 expression, promoting apoptosis and cell cycle arrest of PC cells in response to GEM [31]. In our study, by analyzing the GSE119400 and GSE77310 datasets, we identified HSPA1A, HSPA1B, EFNA4, and HSPB1 as four candidates influenced by hyperthermia in cancer cells. Of these, EFNA4, the only non-HSP family member, piqued our interest for further investigation. We validated that hyperthermia reduced EFNA4 expression in GEM-resistant cell lines. EFNA4 has been implicated as a tumor promoter in various malignancies, including lung cancer [32], gastric cancer [15], hepatocellular carcinoma [33], and breast and ovarian cancers [34]. In PAAD, EFNA4 has also been identified as an important prognostic factor associated with shortened patient survival [35]. However, the role of EFNA4 in PC cell behavior, particularly in GEM resistance, remains poorly understood. Intriguingly, EFNA4 has been reported to promote tumor growth by activating β-catenin [16,33], which has been causatively associated with GEM resistance in PC [7,17]. In our study, we found that artificial overexpression of EFNA4 upregulated β-catenin and downregulated dCK, thereby blocking the GEM-sensitizing effect of hyperthermia. Subsequent treatment with MSAB restored dCK levels and enhanced GEM sensitivity of PC cells, both *in vitro* and *in vivo*, indicating that EFNA4 suppresses dCK activity depending on β-catenin activation.

5. Conclusion

In conclusion, this study elucidates that hyperthermia enhances the therapeutic effect of GEM in PC cells by activating dCK, which is mediated by the suppression of the EFNA4/β-catenin. These findings offer novel insights into the mechanisms underlying the GEM-sensitizing effect of hyperthermia. This enhanced understanding not only strengthens the rationale for incorporating hyperthermia into treatment regimens but provides opportunities for further optimization and refinement of therapeutic strategies. Additionally, the identification of dCK upregulation as a mechanism underlying enhanced GEM sensitivity may have broader implications beyond just the combination with hyperthermia. It could potentially inform the development of novel therapeutic approaches targeting dCK or related pathways to enhance GEM sensitivity, even in the absence of hyperthermia.

Disclosure statement

No potential conflict of interest was reported by the authors.

Data availability statement

Data will be made available on request.

Funding

This work was supported by Natural Science Foundation of Zhejiang Province (Grant LGF21H310004), The Construction Fund of Key Medical Disciplines of Hangzhou (OO20190001) and Key R&D Program of Zhejiang Province (No.2023C03054 No.202403048).

Ethical approval

The animal study protocol was approved by the Animal Ethics Committee of Affiliated Hangzhou First People's Hospital, School of Medicine, Westlake University (Approval No. 2022-1013), and all procedures adhered strictly to the guidelines outlined in the Care and Use of Laboratory Animals (NIH, Bethesda, MD, USA).

CRediT authorship contribution statement

Qiaoxian He: Validation, Methodology, Investigation, Conceptualization. **Yangyang Zheng:** Writing – original draft, Resources, Project administration, Data curation. **Lei Lu:** Writing – original draft, Resources, Methodology, Formal analysis. **Hongzhang Shen:** Writing – original draft, Resources, Project administration, Data curation. **Weigang Gu:** Writing – review & editing, Project administration, Methodology, Formal analysis. **Jianfeng Yang:** Writing – review & editing, Visualization, Methodology, Formal analysis. **Xiaofeng Zhang:** Writing – review & editing, Validation, Supervision, Formal analysis. **Hangbin Jin:** Methodology, Investigation, Funding acquisition, Conceptualization.

Declaration of competing interest

The authors declare that they have no known competing financial interests or personal relationships that could have appeared to influence the work reported in this paper.

Appendix A. Supplementary data

Supplementary data to this article can be found online at https://doi.org/10.1016/j.heliyon.2024.e28488.

References

[1] H. Sung, J. Ferlay, R.L. Siegel, M. Laversanne, I. Soerjomataram, A. Jemal, F. Bray, Global cancer statistics 2020: GLOBOCAN estimates of incidence and mortality worldwide for 36 cancers in 185 countries, CA A Cancer J. Clin. 71 (2021) 209–249.
[2] K. Sriram, C. Salmeron, S.Z. Wiley, P.A. Insel, GPCRs in pancreatic adenocarcinoma: contributors to tumour biology and novel therapeutic targets, Br. J. Pharmacol. 177 (2020) 2434–2455.
[3] R.L. Siegel, K.D. Miller, A. Jemal, Cancer statistics, CA A Cancer J. Clin. 68 (2018) (2018) 7–30.
[4] D. Xie, K. Xie, Pancreatic cancer stromal biology and therapy, Genes Dis 2 (2015) 133–143.
[5] L. de Sousa Cavalcante, G. Monteiro, Gemcitabine: metabolism and molecular mechanisms of action, sensitivity and chemoresistance in pancreatic cancer, Eur. J. Pharmacol. 741 (2014) 8–16.
[6] I. Dufau, C. Frongia, F. Sicard, L. Dedieu, P. Cordelier, F. Ausseil, B. Ducommun, A. Valette, Multicellular tumor spheroid model to evaluate spatio-temporal dynamics effect of chemotherapeutics: application to the gemcitabine/CHK1 inhibitor combination in pancreatic cancer, BMC Cancer 12 (2012) 15.
[7] C. Zhou, C. Yi, Y. Yi, W. Qin, Y. Yan, X. Dong, X. Zhang, Y. Huang, R. Zhang, J. Wei, D.W. Ali, M. Michalak, X.Z. Chen, J. Tang, LncRNA PVT1 promotes gemcitabine resistance of pancreatic cancer via activating Wnt/beta-catenin and autophagy pathway through modulating the miR-619-5p/Pygo2 and miR-619-5p/ATG14 axes, Mol. Cancer 19 (2020) 118.
[8] A. Neesse, P. Michl, K.K. Frese, C. Feig, N. Cook, M.A. Jacobetz, M.P. Lolkema, M. Buchholz, K.P. Olive, T.M. Gress, D.A. Tuveson, Stromal biology and therapy in pancreatic cancer, Gut 60 (2011) 861–868.
[9] Suriyanto, E.Y. Ng, S.D. Kumar, Physical mechanism and modeling of heat generation and transfer in magnetic fluid hyperthermia through Neelian and Brownian relaxation: a review, Biomed. Eng. Online 16 (2017) 36.
[10] H.B. Jin, L. Lu, L. Xie, J.F. Yang, X.F. Zhang, S.L. Ma, Concentration changes in gemcitabine and its metabolites after hyperthermia in pancreatic cancer cells assessed using RP-HPLC, Cell. Mol. Biol. Lett. 24 (2019) 30.
[11] H. Jin, Y. Zhao, J. Yang, X. Zhang, S. Ma, Hyperthermia enhances the sensitivity of pancreatic cancer SW1990 cells to gemcitabine through ROS/JNK signaling, Oncol. Lett. 16 (2018) 6742–6748.
[12] H. Jin, Y. Zhao, S. Zhang, J. Yang, X. Zhang, S. Ma, Hyperthermia inhibits the motility of gemcitabine-resistant pancreatic cancer PANC-1 cells through the inhibition of epithelial-mesenchymal transition, Mol. Med. Rep. 17 (2018) 7274–7280.
[13] S.A. Veltkamp, J.H. Beijnen, J.H. Schellens, Prolonged versus standard gemcitabine infusion: translation of molecular pharmacology to new treatment strategy, Oncol. 13 (2008) 261–276.

[14] S.A. Veltkamp, D. Pluim, M.A. van Eijndhoven, M.J. Bolijn, F.H. Ong, R. Govindarajan, J.D. Unadkat, J.H. Beijnen, J.H. Schellens, New insights into the pharmacology and cytotoxicity of gemcitabine and 2',2'-difluorodeoxyuridine, Mol. Cancer Therapeut. 7 (2008) 2415–2425.
[15] R. Xie, M. Yuan, Y. Jiang, The pan-cancer crosstalk between the EFNA family and tumor microenvironment for prognosis and immunotherapy of gastric cancer, Front. Cell Dev. Biol. 10 (2022) 790947.
[16] J. Lin, C. Zeng, J. Zhang, Z. Song, N. Qi, X. Liu, Z. Zhang, A. Li, F. Chen, EFNA4 promotes cell proliferation and tumor metastasis in hepatocellular carcinoma through a PIK3R2/GSK3beta/beta-catenin positive feedback loop, Mol. Ther. Nucleic Acids 25 (2021) 328–341.
[17] Y.Q. Hua, K. Zhang, J. Sheng, Z.Y. Ning, Y. Li, W.D. Shi, L.M. Liu, Fam83D promotes tumorigenesis and gemcitabine resistance of pancreatic adenocarcinoma through the Wnt/beta-catenin pathway, Life Sci. 287 (2021) 119205.
[18] D. Thummuri, S. Khan, P.W. Underwood, P. Zhang, J. Wiegand, X. Zhang, V. Budamagunta, A. Sobh, A. Tagmount, A. Loguinov, A.N. Riner, A.S. Akki, E. Williamson, R. Hromas, C.D. Vulpe, G. Zheng, J.G. Trevino, D. Zhou, Overcoming gemcitabine resistance in pancreatic cancer using the BCL-X(L)-Specific degrader DT2216, Mol. Cancer Therapeut. 21 (2022) 184–192.
[19] S.Y. Hwang, X. Deng, S. Byun, C. Lee, S.J. Lee, H. Suh, J. Zhang, Q. Kang, T. Zhang, K.D. Westover, A. Mandinova, S.W. Lee, Direct targeting of beta-catenin by a small molecule stimulates proteasomal degradation and suppresses oncogenic wnt/beta-catenin signaling, Cell Rep. 16 (2016) 28–36.
[20] H.J. Chung, H.K. Lee, K.B. Kwon, H.J. Kim, S.T. Hong, Transferrin as a thermosensitizer in radiofrequency hyperthermia for cancer treatment, Sci. Rep. 8 (2018) 13505.
[21] J. van der Zee, Heating the patient: a promising approach? Ann. Oncol. 13 (2002) 1173–1184.
[22] R.D. Issels, Hyperthermia adds to chemotherapy, Eur. J. Cancer 44 (2008) 2546–2554.
[23] Z.W. Lim, V.B. Varma, R.V. Ramanujan, A. Miserez, Magnetically responsive peptide coacervates for dual hyperthermia and chemotherapy treatments of liver cancer, Acta Biomater. 110 (2020) 221–230.
[24] W.P. Tan, A. Chang, S.C. Brousell, D.C. Grimberg, J.J. Fantony, T.A. Longo, W. Etienne, I. Spasojevic, P. Maccarini, B.A. Inman, Safety and efficacy of intravesical chemotherapy and hyperthermia in the bladder: results of a porcine study, Int. J. Hyperther. 37 (2020) 854–860.
[25] A.A. Tentes, K. Stamou, N. Pallas, C. Karamveri, D. Kyziridis, C. Hristakis, The effect of hyperthermic intraoperative intraperitoneal chemotherapy (HIPEC) as an adjuvant in patients with resectable pancreatic cancer, Int. J. Hyperther. 32 (2016) 895–899.
[26] R. Sciarrillo, A. Wojtuszkiewicz, Y.G. Assaraf, G. Jansen, G.J.L. Kaspers, E. Giovannetti, J. Cloos, The role of alternative splicing in cancer: from oncogenesis to drug resistance, Drug Resist. Updates 53 (2020) 100728.
[27] R. Marechal, J.R. Mackey, R. Lai, P. Demetter, M. Peeters, M. Polus, C.E. Cass, I. Salmon, J. Deviere, J.L. Van Laethem, Deoxycitidine kinase is associated with prolonged survival after adjuvant gemcitabine for resected pancreatic adenocarcinoma, Cancer 116 (2010) 5200–5206.
[28] Q. Hu, Y. Qin, J. Xiang, W. Liu, W. Xu, Q. Sun, S. Ji, J. Liu, Z. Zhang, Q. Ni, J. Xu, X. Yu, B. Zhang, dCK negatively regulates the NRF2/ARE axis and ROS production in pancreatic cancer, Cell Prolif. 51 (2018) e12456.
[29] N. Funamizu, A. Okamoto, Y. Kamata, T. Misawa, T. Uwagawa, T. Gocho, K. Yanaga, Y. Manome, Is the resistance of gemcitabine for pancreatic cancer settled only by overexpression of deoxycytidine kinase? Oncol. Rep. 23 (2010) 471–475.
[30] S. Adachi, S. Kokura, T. Okayama, T. Ishikawa, T. Takagi, O. Handa, Y. Naito, T. Yoshikawa, Effect of hyperthermia combined with gemcitabine on apoptotic cell death in cultured human pancreatic cancer cell lines, Int. J. Hyperther. 25 (2009) 210–219.
[31] Y. Guo, A. Ziesch, S. Hocke, E. Kampmann, S. Ochs, E.N. De Toni, B. Goke, E. Gallmeier, Overexpression of heat shock protein 27 (HSP27) increases gemcitabine sensitivity in pancreatic cancer cells through S-phase arrest and apoptosis, J. Cell Mol. Med. 19 (2015) 340–350.
[32] X. Zhao, Y. Chen, X. Sun, Z. He, T. Wu, C. Wu, J. Chen, J. Wang, K. Diao, X.S. Liu, Oncogenic EFNA4 amplification promotes lung adenocarcinoma lymph node metastasis, Cancers 14 (2022).
[33] W. Yuan, H. Zhao, A. Zhou, S. Wang, Interference of EFNA4 suppresses cell proliferation, invasion and angiogenesis in hepatocellular carcinoma by downregulating PYGO2, Cancer Biol. Ther. 23 (2022) 1–12.
[34] M. Damelin, A. Bankovich, A. Park, J. Aguilar, W. Anderson, M. Santaguida, M. Aujay, S. Fong, K. Khandke, V. Pulito, E. Ernstoff, P. Escarpe, J. Bernstein, M. Pysz, W. Zhong, E. Upeslacis, J. Lucas, J. Lucas, T. Nichols, K. Loving, O. Foord, J. Hampl, R. Stull, F. Barletta, H. Falahatpisheh, P. Sapra, H.P. Gerber, S. J. Dylla, Anti-EFNA4 calicheamicin conjugates effectively target triple-negative breast and ovarian tumor-initiating cells to result in sustained tumor regressions, Clin. Cancer Res. 21 (2015) 4165–4173.
[35] I. Khatri, M.K. Bhasin, A transcriptomics-based meta-analysis combined with machine learning identifies a secretory biomarker panel for diagnosis of pancreatic adenocarcinoma, Front. Genet. 11 (2020) 572284.